

NiO as an Inorganic Hole-Transporting Layer in Quantum-Dot Light-Emitting Devices

Jean-Michel Caruge,[†] Jonathan E. Halpert,[†] Vladimir Bulović,^{*,‡} and Mounji G. Bawendi^{*,†}

Department of Chemistry, Massachusetts Institute of Technology, 77 Massachusetts Avenue, Cambridge, Massachusetts 02139, Laboratory of Organic Optics and Electronics, Department of Electrical Engineering and Computer Science, Massachusetts Institute of Technology, 77 Massachusetts Avenue, Cambridge, Massachusetts 02139

Received October 2, 2006

ABSTRACT

We demonstrate a hybrid inorganic/organic light-emitting device composed of a CdSe/ZnS core/shell semiconductor quantum-dot emissive layer sandwiched between p-type NiO and tris(8-hydroxyquinoline) aluminum (Alq₃), as hole and electron transporting layers, respectively. A maximum external electroluminescence quantum efficiency of 0.18% is achieved by tuning the resistivity of the NiO layer to balance the electron and hole densities at quantum-dot sites.

Advances in the chemical synthesis and processing of colloidal semiconductor quantum dots (QDs) combined with the unique emissive properties of these inorganic nanomaterials have triggered the development of QD light-emitting devices (QD-LEDs). Recent works have focused on the choice of adequate electron- and hole-transporting layers to realize high-performance QD-LEDs emitting in the near-infrared and visible spectral ranges.^{1–5} To date, the most efficient QD-LED reported⁵ in the visible spectrum was a hybrid QD/organic device composed of a monolayer of closely packed CdSe/ZnS core/shell QDs sandwiched between organic *N,N'*-diphenyl-*N,N'*-bis(3-methylphenyl)-1-1'-biphenyl-4,4'-diamine (TPD) and tris(8-hydroxyquinoline) aluminum (Alq₃) hole and electron transporting layers, respectively. At video brightness, the external electroluminescence (EL) quantum efficiency (η_{EL}) of these devices was ~2%.⁵ To be applicable in display and lighting applications, QD-LEDs not only must be efficient but must also have long operating lifetimes. The lifetime of a typical ITO/TPD/QD/Alq₃/Mg:Ag/Ag device is limited, as in OLEDs, by the degradation of the organic layers under moisture and oxygen and the instability of the metal contacts.^{6,7}

In this work, we explore the possibility of replacing the TPD film with a high-band-gap (>3 eV) inorganic hole-

transporting layer that is chemically and electrically more stable. NiO has been selected from band-offset considerations (relative to CdSe QDs), ease of deposition, and its chemical compatibility with the CdSe QDs. Additionally, early studies have shown that transparent p-type NiO thin films can be obtained by near-room-temperature reactive sputtering of NiO or Ni targets and can be used as hole-transporting/injecting layers in electro-optical devices.^{8–10} The QD-LED structure we investigate is sketched in the band diagram in Figure 1a with a NiO hole-transporting layer and an Alq₃ electron-transporting layer sandwiching the QD lumophores.

The quenching of QD electroluminescence by the high density of free charge carriers in NiO and the balance^{11–14} of electron and hole currents are two crucial challenges that have to be overcome in order to build efficient NiO QD-LEDs.

We first address the quenching mechanism by observing that photoluminescence intensities of single QDs deposited onto resistive ($\rho \approx 1 \Omega \cdot \text{cm}$) NiO thin films remain high, in contrast to quenched photoluminescence of single QDs deposited onto highly conductive ($\rho \approx 5 \times 10^{-4} \Omega \cdot \text{cm}$) NiO thin films. The same observation was made for a 30-nm-thick close-packed QD film deposited by spin-coating onto resistive and highly conductive NiO. These observations are consistent with early theoretical and experimental works,^{15–19} which demonstrated that photoluminescence quenching of organic and inorganic lumophores by a conductive dielectric via an energy-transfer process can be tuned by controlling

* Corresponding authors. E-mail: bulovic@mit.edu; mgb@mit.edu.

[†] Department of Chemistry.

[‡] Laboratory of Organic Optics and Electronics, Department of Electrical Engineering and Computer Science.

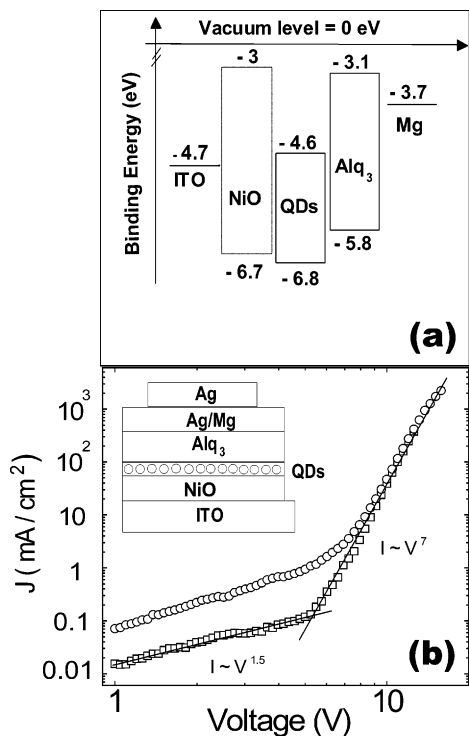


Figure 1. (a) Proposed band diagram of a NiO QD-LED. (b) Forward-biased current–voltage characteristics for NiO QD LEDs constructed with high-resistivity (open squares) and low-resistivity (open circles) NiO HTLs. The contact area is 0.78 mm^2 for both devices. Inset: schematic representation of the QD-LED structure.

the chromophore–dielectric distance and by tuning the electrical permittivity of the dielectric, which in our study changes with the hole density in the NiO layer. In the case of EL, upon an applied voltage, accumulation of holes around the QD layer, due to the presence of energy barriers, will induce fluctuations in the local hole density, which could affect the quenching of the EL from QDs. However, we believe that the -0.1 and 1 eV band offsets (Figure 1a) at the NiO/QD and QD/Alq₃ interfaces should easily facilitate hole injection into the QDs and Alq₃ (in forward bias) and that a drastic change in the local hole density is unlikely to occur.

Second, we show below that the control of the oxygen concentration inside the sputtering chamber during the sputtering step enables us to accurately tune the resistivity of the NiO films and improve the charge balance inside our devices.

In the following sections, we start by describing the fabrication process of the NiO QD-LEDs. We then show that space-charge-limited conduction is the dominant charge conduction mechanism and demonstrate that η_{EL} up to 0.18% can be achieved in our devices.

The NiO QD-LEDs were fabricated as follows: Prior to the deposition of the NiO thin films, ITO precoated (150 nm thick) glass substrates (with sheet resistance of $30 \text{ } \Omega$ per square) were cleaned via sequential ultrasonic rinses in detergent solution, deionized water, and acetone and then boiled in isopropanol for 5 min. After cleaning, the glass substrates were dried in nitrogen and exposed to UV-ozone

to eliminate any adsorbed organic materials. They were then inserted into a nitrogen glove box, which is connected to a sputtering and evaporation chamber via a high vacuum transfer line. In the sputtering chamber, a 30-nm-thick NiO thin film was deposited by reactive RF magnetron sputtering of a NiO target in an Ar/O₂ gas mixture. For our most efficient QD-LED described in this paper, the base pressure before sputtering was 10^{-7} Torr, the RF power was fixed at 200 W, the plasma pressure was 6 mTorr, and the ratio between the O₂ and Ar gas flow rates was 2.5%, which, with our sputtering geometry, resulted in a NiO deposition rate of 0.03 nm/s. With the above deposition parameters, the NiO thin films showed p-type conductivity with resistivity of $\rho = 5 \text{ } \Omega \cdot \text{cm}$ (sheet resistance of $2 \text{ M}\Omega$ per square), and optical transmission of 80% at $\lambda = 625 \text{ nm}$ (center of the QD emission peak). The resistivity of the p-type NiO thin films is tuned accurately by varying the ratio between the O₂ and Ar flow rates: higher oxygen concentration in the sputtering chamber gives lower resistivities. For instance, increasing the oxygen to argon gas ratio from 2.5% to 10% decreases the resistivity of NiO films from $\rho = 5 \text{ } \Omega \cdot \text{cm}$ to $\rho = 5 \times 10^{-4} \text{ } \Omega \cdot \text{cm}$. AFM characterizations of the ITO/NiO surface reveals a rms surface roughness of $\sim 2 \text{ nm}$. The surface roughness comes mainly from the ~ 150 -nm-thick commercial ITO films. Indeed, AFM images of a 30-nm-thick NiO thin film sputtered (with the same deposition parameters) onto a flat glass substrate reveal an rms surface roughness of 0.3 nm. Of paramount importance, the NiO films were also highly stable in air and in the presence of the organic solvents used during chemical processing of the QDs.

The glass/ITO/NiO substrates were transferred back into the glove box where they were coated with a 20-nm-thick layer of CdSe/ZnS core/shell QDs that was spun-cast out of chloroform. The thickness of the spun-cast QD films can be tuned by varying the QD concentration in chloroform and/or the spin speed during the spin-coating process. The substrates were then transferred, without exposure to air, into the evaporation chamber, and a 40-nm-thick Alq₃ electron-transporting layer was evaporated at 10^{-6} Torr, at a deposition rate of $\sim 0.2 \text{ nm/s}$. A 100-nm-thick Ag/Mg (1/10 by weight) and 30-nm-thick Ag electron-injecting electrode were then evaporated through a shadow mask, forming 1-mm-diameter circular electrodes. The freshly made QD-LEDs were removed from the integrated deposition system, without packaging, and immediately tested in air.

Two sets of devices, with $\rho_1 = 5 \text{ } \Omega \cdot \text{cm}$ (high-resistivity NiO) and $\rho_2 = 10^{-2} \text{ } \Omega \cdot \text{cm}$ (low-resistivity NiO), were investigated in this paper. Typical forward biased current–voltage (I – V) characteristics for the two sets of devices (measured with respect to the grounded Ag cathode) are plotted in Figure 1b. The open square and open circle curves are typical I – V curves for the high- and low-resistivity devices, respectively. For both sets of devices, $J \propto V^n$ with $1 < n < 1.5$ below $\sim 6 \text{ V}$ and $6 < n < 7$ at higher voltages. Here, n is the signature of the charge conduction mechanism and is related to the temperature and to the density and energy distribution of trap states in the organic or inorganic

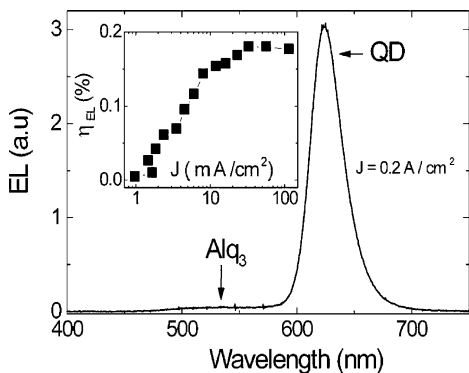


Figure 2. EL spectrum of a NiO QD-LED taken from a high-resistivity NiO device at a current density of 200 mA/cm². More than 95% of the EL originates from QD luminescence. The resistivity of the NiO thin film is 5 Ω·cm. The fwhm of the QD emission peak is 30 nm. The spectral shoulder at $\lambda = 530$ nm is due to Alq₃ emission. Inset: external electroluminescence quantum efficiency vs current density for the same NiO QD-LED.

materials. These I – V curves are consistent with previous reports of trap-assisted space-charge-limited conduction in both CdSe/ ZnS⁴ close packed films and OLEDs.^{20,21} The turn-on voltage, defined as the minimum voltage for which EL can be detected from the devices with an Ocean Optics (SD 2000) spectrometer, is between 6 and 7 V for both sets of devices. The maximum steady-state current densities achieved in the high- and low-resistivity devices are 300 mA/cm² and ~ 4000 mA/cm², respectively. At these current densities, 6×10^6 and 8×10^7 carriers per second, respectively, can be injected into each QD within the luminescent QD layer. Because the single exciton recombination time in a QD is ≤ 10 ns,^{22,23} at these current levels the maximum exciton density per QD is 3% and 40% for the high- and low-resistivity devices, respectively.

Figure 2 shows the EL spectrum of a NiO QD-LED, containing a resistive NiO layer ($\rho_1 = 5$ Ω·cm), at a current density of 200 mA/cm². The 30 nm fwhm QD emission peak centered at $\lambda = 625$ nm dominates the EL spectrum. The broader shoulder centered at $\lambda = 530$ nm is due to a weak Alq₃ emission. The 1 eV band offset (Figure 1a) between the HOMO levels of CdSe QDs and Alq₃ enables hole injection into the Alq₃ film. The inset in Figure 2 shows the evolution of η_{EL} as a function of current density for the same device. The efficiency is calculated as the ratio between the measured photocurrent (measured with a calibrated silicon photodetector) and the total injected current into the device. A maximum η_{EL} of 0.18% and brightness of up to 3000 cd/m² are achieved for most of the high-resistivity devices.

Figure 3 illustrates the negative impact of low-resistance NiO (10^{-2} Ω·cm) on the QD-LED EL spectrum for the second set of devices. In contrast to the device in Figure 2, nearly 50% of the detected EL comes from the Alq₃ layer for current densities lower than 300 mA/cm². This effect is attributed to (i) the imbalance of electron and hole injection at QD sites due to the highly doped NiO thin films, which decreases the exciton density per QD, and (ii) the quenching of the QD layer by the free holes in NiO via energy transfer. Additionally, previous studies on the photoluminescence

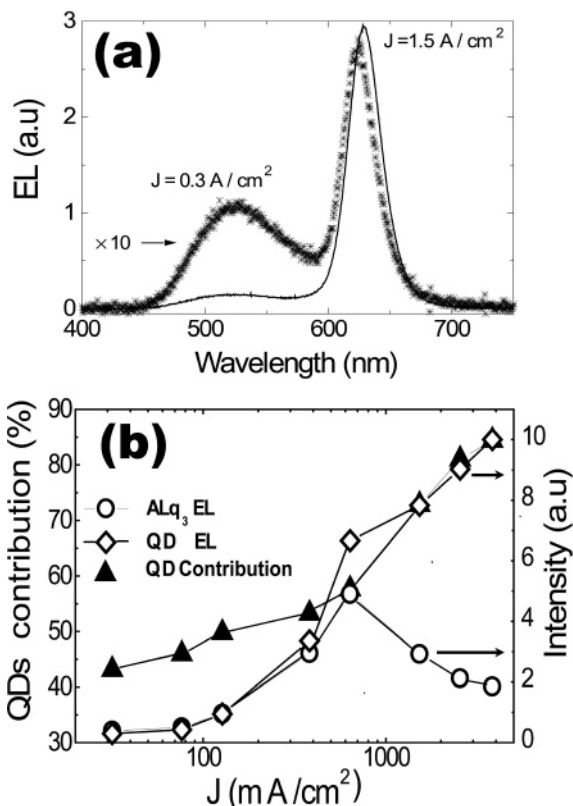


Figure 3. (a) EL spectra of a NiO QD-LED at 300 mA/cm² (stars) and 1500 mA/cm² (solid line) using a film with a resistivity of 10^{-2} Ω·cm. (b) Contribution (solid triangles) of the QD electro-luminescence to the EL spectrum versus current density. Integrated areas below the Alq₃ (open circles) and QD (open diamonds) emission peaks, in arbitrary units, as a function of the current density.

intermittency of single CdSe QDs^{24–27} and charging²⁸ of self-assembled CdSe QD films have shown that a charged QD (i.e., a QD with an excess of holes or electrons) is non-emissive because of ultrafast (~ 100 ps) nonradiative Auger^{29–30} processes. Furthermore, the increased hole density shifts the exciton recombination region into the Alq₃ layer, which leads to more emission from the organic layer. At 1.5 A/cm², 85% of the EL originates from the QDs. The increase in the QD spectral contribution with current is due to a 60% decrease in the Alq₃ emission from 600 mA/cm² to 3000 mA/cm² combined with a 50% increase in the QD emission. Figure 3b illustrates the evolution of the integrated areas below the Alq₃ and QD EL peaks, respectively. The solid triangle curve summarizes the evolution of the spectral contribution (in %) of the QDs to the EL spectrum as a function of current density. A 5 nm red shift is noticeable in the EL spectrum at 1.5 A/cm². We speculate that this is due to a Stark effect from high local fields at high current densities.

Finally, as a consequence of quenching and charge imbalance, $\eta_{EL} < 10^{-3}$ % for most of the devices using low-resistivity NiO.

In conclusion, we have fabricated QD-LEDs using p-type NiO films as hole-transporting layers. Careful optimization of the NiO thin film resistivity has enabled us to (i) reduce the quenching of QD luminescence (ii) improve the charge

balance inside the device and (iii) reach QD-LED external quantum efficiencies of 0.18%. The present QD-LEDs are less efficient than the best reported QD-LEDs that utilize TPD hole transport layer. In contrast to earlier studies, however, this work utilizes more stable metal oxide films. Furthermore, we believe that we have not yet reached the limit of device optimization because we speculate that a large fraction of the injected current is shunted through the device due to the roughness of the ITO/NiO sputtered interface. With a smoother ITO/NiO interface, we expect to increase the QD-LED efficiency due to the reduction of shunt currents from direct contacts between ITO/NiO spikes and the Alq₃ layer. Finally, the use of a stable inorganic material as the hole-injection layer enables deposition of QDs by spin-casting or even inkjet-printing out of organic solutions. This is in contrast to solvent-sensitive organic thin films, which require more complicated stamping deposition techniques.³¹ Consequently, the introduction of metal oxides has expanded and simplified the fabrication process of QD-LEDs.

Acknowledgment. This research was funded in part by the NSF-MRSEC program (DMR-0213282), making use of its shared experimental facilities, a PECASE grant (VB), and by the U.S. Army through the Institute for Soldier Nanotechnologies (DAAD-19-02-0002). MGB also acknowledges funding from the David and Lucile Packard Foundation and the Harrison Spectroscopy Laboratory (NSF-CHE-011370).

References

- (1) Colvin, V. L.; Schlamp, M. C.; Alivisatos, A. P. *Nature* **1994**, *370*, 354.
- (2) Tessler, N.; Medvedev, V.; Kazes, M.; Kan, S.; Banin, U. *Science* **2002**, *295*, 1506.
- (3) Coe-Sullivan, S.; Woo, W.-K.; Bawendi, M.; Bulovic, V. *Nature* **2002**, *420*, 800.
- (4) Hikmet, R. A. M.; Talapin, D. V.; Heller, H. *J. Appl. Phys.* **2003**, *93*, 3509.
- (5) (a) Coe-Sullivan, S.; Steckel, J. S.; Woo, W.-K.; Bawendi, M. G.; Bulovic, V. *Adv. Funct. Mater.* **2005**, *15*, 1117–1124. (b) Coe-Sullivan, S.; Woo, W.-K.; Steckel, J.; Bawendi, M. G.; Bulovic, V. *Org. Electron.* **2003**, *4*, 123–130.
- (6) Gosh, A. P.; Gerenser, L. J.; Jarman, C. M.; Formalik, J. E. *Appl. Phys. Lett.* **2005**, *86*, 223503.
- (7) McElvain, J. M.; Antoniadis, H.; Hueschen, M. R.; Miller, J. N.; Roitman, D. M.; Sheats, J. R.; Moon, R. L. *J. Appl. Phys.* **1996**, *80*, 6002.
- (8) Sato, H.; Minami, T.; Takata, S.; Yamada, T. *Thin Solid Films* **1993**, *236*, 1–2.
- (9) Suga, K.; Koshizaki, N.; Yasumoto, K.; Smela, E. *Sens. Actuators, B* **1993**, *14*, 598.
- (10) Lee, W. Y.; Mauri, D.; Hwang, C. *Appl. Phys. Lett.* **1998**, *72*, 1584.
- (11) Liao, C.-H.; Lee, M.-T.; Tsai, C.-H.; Chen, C. H. *Appl. Phys. Lett.* **2005**, *86*, 203507.
- (12) VanSlyke, S. A.; Chen, C. H.; Tang, C. W. *Appl. Phys. Lett.* **1996**, *69*, 2160.
- (13) Aziz, H.; Popovic, Z. D.; Hu, N.-X.; Hor, A.-M.; Xu, G. *Science* **1999**, *283*, 1900.
- (14) Aziz, H.; Popovic, Z. D. *Appl. Phys. Lett.* **2002**, *80*, 2180.
- (15) Drexhage, K. H.; Fleck, M.; Khun, H.; Schaffer, F. P.; Sperling, W. *Ber. Bunsen-Ges. Phys. Chem.* **1966**, *70*, 1179.
- (16) Kuhn, H.; Mobius, D. *Angew. Chem.* **1971**, *10*, 620.
- (17) Chance, R. R.; Prock, A.; Silbey, R. *J. Chem. Phys.* **1974**, *60*, 2744.
- (18) Larkin, I.; Stockma, M. I.; Achermann, M.; Klimov, V. *Phys. Rev. B* **2004**, *69*, 121403(R).
- (19) Morawitz, H. *Phys. Rev.* **1969**, *187*, 1792.
- (20) Burrows, P. E.; Forrest, S. R. *Appl. Phys. Lett.* **1994**, *64*, 2285.
- (21) Burrows, P. E.; Shen, Z.; Bulovic, V.; McCarty, D. M.; Forrest, S. R.; Cronin, J. E.; Thompson, M. E. *J. Appl. Phys.* **1996**, *79*, 7991.
- (22) Brokmann, X.; Coolen, L.; Dahan, M.; Hermier, J. P. *Phys. Rev. Lett.* **2004**, *93*, 107403.
- (23) Kagan, C. R.; Murray, C. B.; Nirmal, M.; Bawendi, M. G. *Phys. Rev. Lett.* **1996**, *76*, 1517.
- (24) Nirmal, M.; Dabbousi, B. O.; Bawendi, M. G.; Macklin, J. J.; Trautman, J. K.; Harris, T. D.; Brus, L. E. *Nature (London)* **1996**, *383*, 802.
- (25) Neuhauser, R. G.; Shimizu, K. T.; Woo, W. K.; Empedocles, S. A.; Bawendi, M. G. *Phys. Rev. Lett.* **2000**, *85*, 3301.
- (26) Tang, J.; Marcus, R. A. *J. Chem. Phys.* **2005**, *123*, 054704.
- (27) Krauss, T. D.; Brus, L. E. *Phys. Rev. Lett.* **1999**, *83*, 4840.
- (28) Woo, W. K.; Shimizu, K. T.; Jarosz, M. V.; Neuhauser, R. G.; Leatherdale, C. A.; Rubner, M. A.; Bawendi, M. G. *Adv. Mater.* **2002**, *14*, 1071.
- (29) Kharchenko, V. A.; Rosen, M. J. *Lumin.* **1996**, *70*, 158.
- (30) Guyot-Sionnest, P.; Wehrenberg, B.; Yu, D. *J. Chem. Phys.* **2005**, *123*, 074709.
- (31) Steckel, J. S.; Snee, P.; Coe-Sullivan, S.; Zimmer, J. P.; Halpert, J. E.; Anikeeva, P.; Kim, L.-A.; Bulovic, V.; Bawendi, M. G. *Angew. Chem., Int. Ed.* **2006**, *45*, 5796.

NL0623208